



Structural connectivity reproducibility through multiple acquisitions

Gabriel Girard, Kevin Whittingstall, Rachid Deriche, Maxime Descoteaux

► To cite this version:

Gabriel Girard, Kevin Whittingstall, Rachid Deriche, Maxime Descoteaux. Structural connectivity reproducibility through multiple acquisitions. Organization for Human Brain Mapping, Jun 2015, Honolulu, United States. hal-01174327

HAL Id: hal-01174327

<https://hal.inria.fr/hal-01174327>

Submitted on 8 Jul 2015

HAL is a multi-disciplinary open access archive for the deposit and dissemination of scientific research documents, whether they are published or not. The documents may come from teaching and research institutions in France or abroad, or from public or private research centers.

L'archive ouverte pluridisciplinaire **HAL**, est destinée au dépôt et à la diffusion de documents scientifiques de niveau recherche, publiés ou non, émanant des établissements d'enseignement et de recherche français ou étrangers, des laboratoires publics ou privés.

Structural connectivity reproducibility through multiple acquisitions

Submission Number:

5730

Submission Type:

Abstract Submission

Authors:

Gabriel Girard¹, Kevin Whittingstall¹, Rachid Deriche², Maxime Descoteaux¹

Institutions:

¹Université de Sherbrooke, Sherbrooke, Québec, ²INRIA, Sophia-Antipolis, France

Introduction:

Diffusion-weighted imaging is often used to reconstruct white matter (wm) pathways between brain areas for in vivo brain connectivity. In this study, we investigate the reproducibility and the specificity of connectivity matrices [Hagmann et al, 2007] in cortico-cortical connectivity using probabilistic and deterministic streamline tractography, seeding from both the wm and the wm-grey matter (gm) interface.

Methods:

Diffusion-weighted images were acquired on 3 volunteers (V1, V2, V3) along 64 uniformly distributed directions using a b-value of 1000 s/mm², a single-shot echo-planar imaging sequence on a 1.5 Tesla SIEMENS Magnetom (128×128 matrix, 2 mm isotropic resolution, TR/TE 11000/98 ms) and a GRAPPA factor of 2. An additional b0 image was acquired in reversed phase-encode direction to correct for susceptibility-induced distortions using FSL/TOPUP [Andersson et al., 2003]. An anatomical T1-weighted 1 mm isotropic MPRAGE (TR/TE 6.57/ 2.52 ms) image was also acquired. The whole sequence was repeated 4 times (A1, A2, A3, A4) for each volunteer (twice with delay of 10 minutes, twice with a delay of 2 days).

The T1-weighted image was linearly registered to an upsampled b0 image using FSL/FLIRT [Jenkinson and Smith, 2001]. Freesurfer [Fischl et al., 2004] was then used to parcelate the registered T1-weighted image into 150 cortical regions [Destrieux et al, 2009], which were used to compute the connectivity matrix **C**. Fiber orientation distribution functions were computed using MRtrix [Tournier et al., 2012] and used for tractography. Partial volume estimation maps from the T1-weighted image were obtained using FSL/Fast [Zhang et al., 2001] and used in the tracking process to enforce gm to gm connectivity [Girard et al., 2014]. Streamlines were generated by seeding from both the wm (5 seeds per voxel) and the wm-gm interface (10 seeds per voxel). In each dataset, the connectivity matrix **C** was defined as the number of streamlines connecting pairs of regions and computed using Dipy [Garyfallidis et al., 2014]. These were then normalized to account for various streamline counts. The difference between 2 connectivity matrices was computed as $d = \sum |C_1 - C_2| / 2$. Thus, **d** is the fraction of streamlines connecting different regions in both matrices.

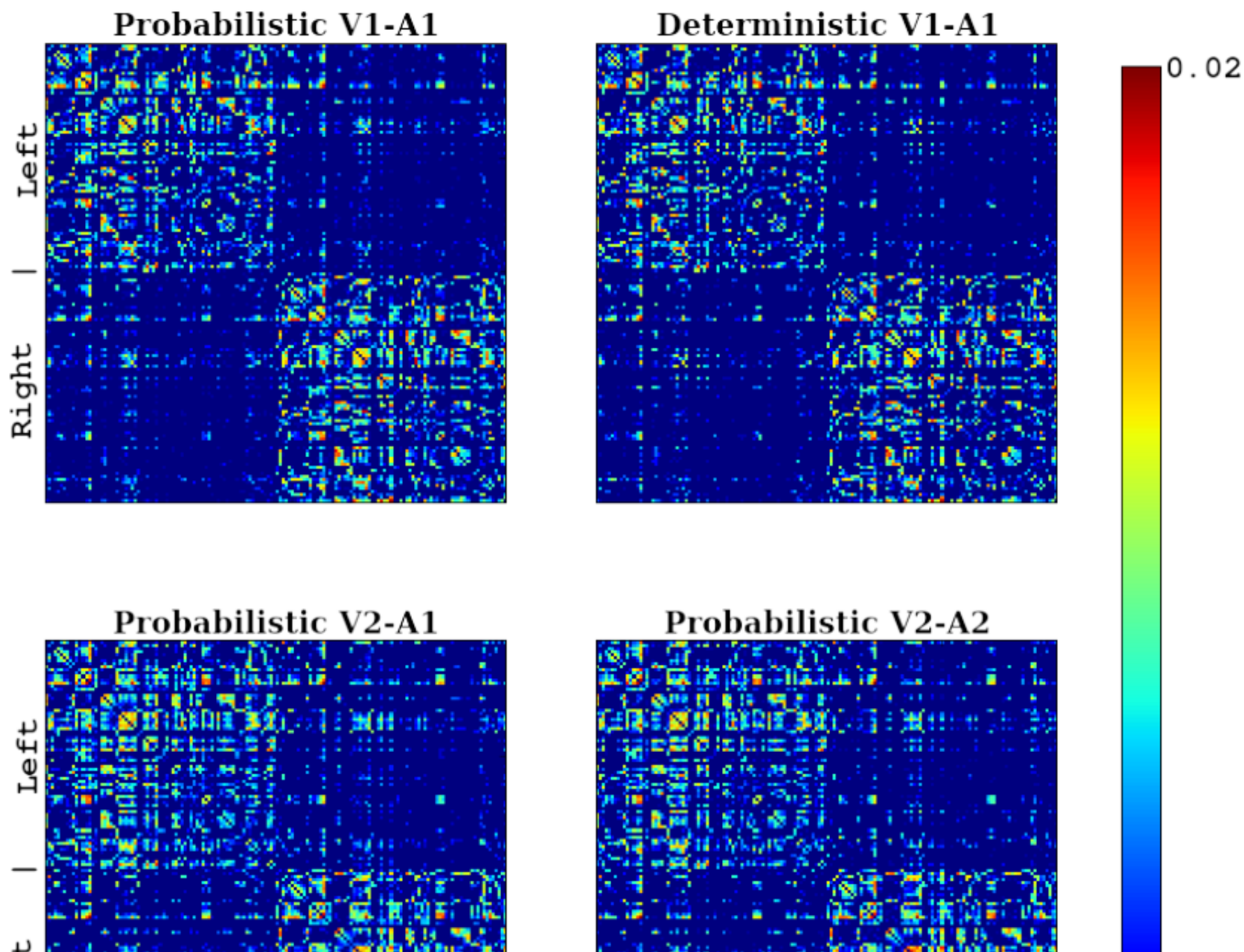
We used the Dunn index (DI) [Dunn, 1973] to evaluate both the intra-subject similarity of the connectivity matrices and the inter-subject differences. DI is computed as the average distance of intra-subject connectivity matrices over the average distance of inter-subject connectivity matrices.

Results:

Fig. 1 shows example connectivity matrices. Fig. 2 shows the distances between each matrix of the 4 pipelines and Table 1 shows their associated DI.

Connectivity matrices (see Fig. 1) show consistency for both inter- and intra- subject distances (see Fig. 2). Probabilistic tractography have a higher DI (1.63) than deterministic tractography (1.39). Interface seeding produces both a lower inter- and intra-subject distances than wm seeding. Furthermore, interface seeding is preferable to wm seeding since it limits the bias in the streamline distribution introduced by the over seeding in longer bundles [Girard et al., 2014, Hagmann et al., 2007]. Overall, the probabilistic wm-gm interface tractography has an average of 16.8% of streamlines connecting different brain regions for

intra-subject reconstructions, 27.3% for inter-subject reconstructions. Hence, our results show that one's connectivity matrix could be recognized amongst a set of individual's connectivity matrices and as such, could be useful to identify group differences.



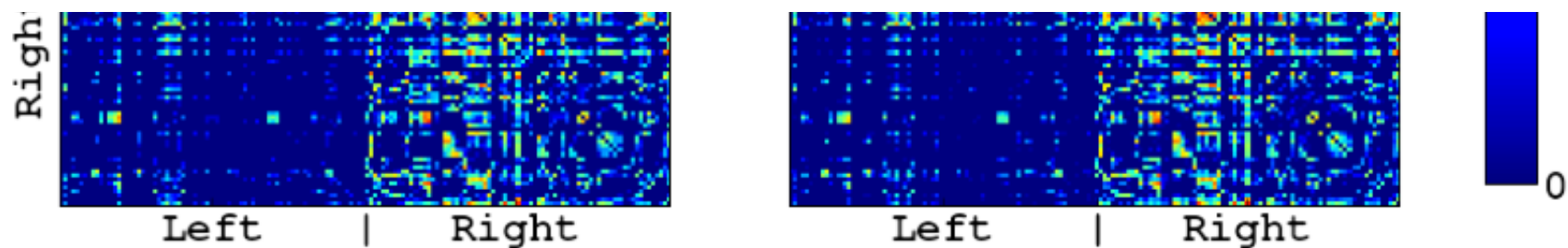
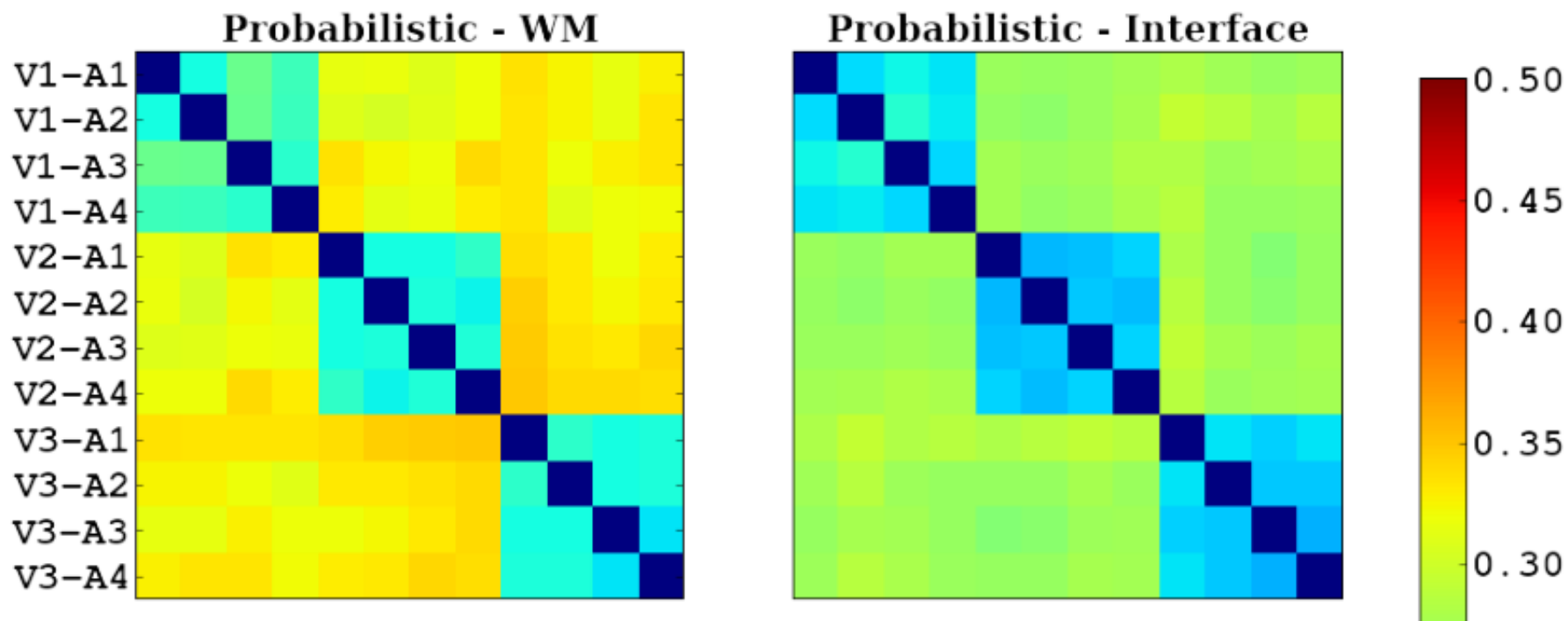


Figure 1: Connectivity matrices using wm-gm interface seeding. The first row shows connectivity matrices of deterministic and probabilistic tractography for the same subject and acquisition. The second row shows the connectivity matrices of probabilistic tractography for 2 acquisitions of the same subject. Differences in the connectivity matrices can be observed between probabilistic and deterministic tractography, and between both subjects probabilistic tractography.



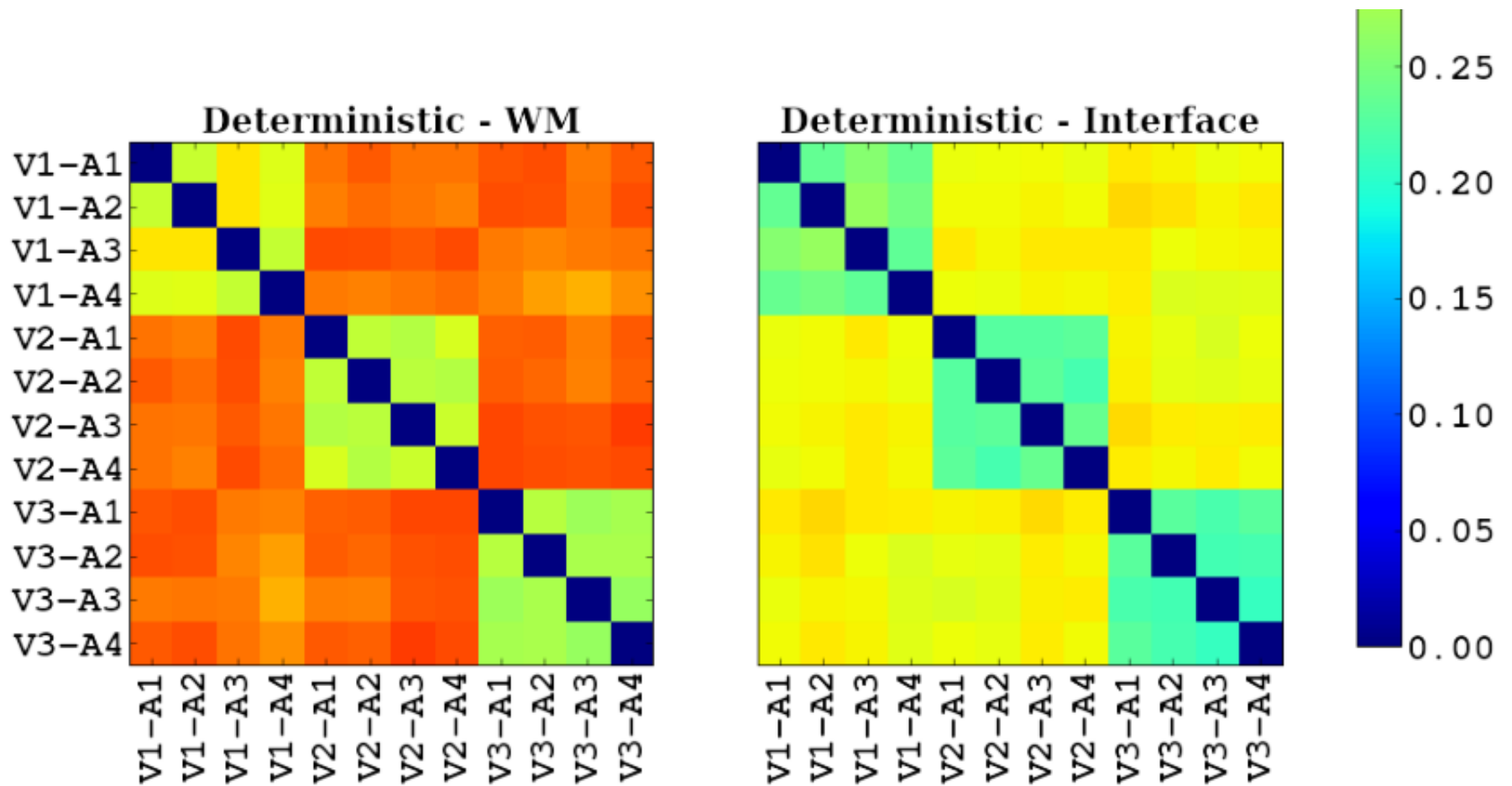


Figure 2: Distances between connectivity matrices. The distance between 2 connectivity matrices C_i is computed as $\sum |C_1 - C_2|/2$. The first row shows the probabilistic tractography pipelines and the second row the deterministic tractography pipelines. Distance ranges vary among pipelines, but consistently shows lower values for intra-subject than inter-subject connectivity matrices.

	Tractography			
	Deterministic		Probabilistic	
	WM	Interface	WM	Interface
Inter-subject distance	39.9%	32.3%	32.7%	27.3%
Intra-subject distance	29.4%	23.2%	19.9%	16.8%
Dunn index	1.36	1.39	1.64	1.63

Table 1: Connectivity matrix analysis. The distance between 2 connectivity matrices C_i is computed as $\sum |C_1 - C_2|/2$. The inter-subject distance is computed as the average distance between pairs of matrices of different brains. The intra-subject distance is computed as the average distance between pairs of matrices of the same brain. The Dunn index (DI) is the ratio of inter- to intra-subject distances. Probabilistic tractography shows a higher DI than deterministic tractography. Wm-gm interface seeding reduces both the intra- and inter-subject distances compared to wm seeding.

Conclusions:

In this study, we showed that with the chosen acquisition scheme, probabilistic tractography produces connectivity matrices with the highest ratio of inter- to intra-subject distances. Moreover, we showed that connectivity matrices may be used as a tool to compare tractography algorithms in terms reproducibility and specificity.

Imaging Methods:

Diffusion MRI ²

Neuroanatomy:

White Matter Anatomy, Fiber Pathways and Connectivity ¹

Keywords:

MRI

Tractography

WHITE MATTER IMAGING - DTI, HARDI, DSI, ETC

^{1/2}*Indicates the priority used for review*

Would you accept an oral presentation if your abstract is selected for an oral session?

Yes

Please indicate below if your study was a "resting state" or "task-activation" study.

Other

Healthy subjects only or patients (note that patient studies may also involve healthy subjects):

Healthy subjects

Internal Review Board (IRB) or Animal Use and Care Committee (AUCC) Approval. Please indicate approval below. Please note: Failure to have IRB or AUCC approval, if applicable will lead to automatic rejection of abstract.

Yes, I have IRB or AUCC approval

Please indicate which methods were used in your research:

Structural MRI

Diffusion MRI

For human MRI, what field strength scanner do you use?

1.5T

Which processing packages did you use for your study?

FSL

Free Surfer

Other, Please list - Dipy

Provide references in author date format

Andersson, J. L. R., Skare, S., & Ashburner, J. (2003). How to correct susceptibility distortions in spin-echo echo-planar images: application to diffusion tensor imaging. *NeuroImage*, 20(2), 870–88.

Destrieux, C., Fischl, B., Dale, A., & Halgren, E. (2010). Automatic parcellation of human cortical gyri and sulci using standard anatomical nomenclature. *NeuroImage*, 53(1), 1–15.

Dunn, J. C. (1973). A Fuzzy Relative of the ISODATA Process and Its Use in Detecting Compact Well-Separated Clusters. *Journal of Cybernetics*, 3 (3), 32–57.

Fischl, B. (2004). Automatically Parcellating the Human Cerebral Cortex. *Cerebral Cortex*, 14(1), 11–22.

Garyfallidis, E., Brett, M., Amirbekian, B., Rokem, A., Van Der Walt, S., Descoteaux, M., & Nimmo-Smith, I. (2014). Dipy, a library for the analysis of diffusion

MRI data. *Frontiers in Neuroinformatics*, 8.

Girard, G., Whittingstall, K., Deriche, R., & Descoteaux, M. (2014). Towards quantitative connectivity analysis: reducing tractography biases. *NeuroImage*, 98, 266–278.

Hagmann, P., Kuran, M., Gigandet, X., Thiran, P., Wedeen, V. J., Meuli, R., & Thiran, J.-P., Jan. (2007). Mapping human whole-brain structural networks with diffusion MRI. *PLoS one* 2 (7).

Jenkinson, M., & Smith, S. (2001). A global optimisation method for robust affine registration of brain images. *Medical Image Analysis*, 5(2), 143–156.

Tournier, J.-D., Calamante, F., & Connelly, A. (2012). MRtrix: Diffusion tractography in crossing fiber regions. *International Journal of Imaging Systems and Technology*, 22(1), 53–66.

Zhang, Y., Brady, M., & Smith, S. (2001). Segmentation of brain MR images through a hidden Markov random field model and the expectation-maximization algorithm. *IEEE Transactions on Medical Imaging*, 20(1), 45–57.